Copper Oxide as an Oxygen Carrier for Chemical Looping Combustion

Eli A. Goldstein and Reginald E. Mitchell

High Temperature Gasdynamics Laboratory
Thermosciences Group
Mechanical Engineering Department
Stanford University
Palo Alto, CA 94305

Abstract

Copper II oxide (CuO) has been investigated as an oxygen carrier for a chemical looping combustion system with a variety of fuels: CO, H_2 and CH_4. Preliminary experiments were performed in a single-pass, bench-scale atmospheric pressure flow reactor as well as in a thermogravimetric analyzer. In the flow reactor experiments, 5 to 10 grams of CuO were loaded into the reactor and the gaseous fuel or argon was admitted at a flow rate of 150 - 300 milliliters per minute. The temperature of the entering gas was increased from room temperature to about 1000 ˚C at a rate between 5 and 12 degrees per minute during each experiment, and the mole fractions of CO, CO_2, H_2, CH_4, and O_2 in the gases evolved from the reactor were measured via gas chromatography. After selected experiments, the solids were examined via scanning electron microscopy and x-ray diffraction spectroscopy, which indicated the reduction of CuO to Cu_2O and Cu.

Oxidation experiments were also performed in a thermogravimetric analyzer (TGA) when CO was the fuel. In these experiments, about 40 mg of CuO were placed on the balance pan of the TGA and mixtures of CO in nitrogen at selected temperatures and pressures were admitted into the reaction chamber of the TGA. The data obtained (changes in weight of the metal oxide as a function of time) were used to develop a reduced chemical reaction mechanism for the oxidation of CO with CuO.

Our results indicate that CuO is an ideal oxygen carrier candidate for chemical looping combustion applications with a variety of fuels. There appear to be no kinetic limitations.

Introduction

Since coal is the cheapest and most abundant fuel in the United States, it is the primary energy source used for electric power generation, and it will continue to be used in such a manner until non-fossil-fuel based technologies for electric power generation are commercially proven and in relatively widespread use. Clean coal technologies have been developed to the point where the emissions of NO_x, SO_x, particulate matter and mercury from present-day coal-fired power plants are below all regulated levels, however carbon dioxide emissions are quite high. Since CO_2 is a greenhouse gas, it is prudent to remove it from power plant exhaust streams before it is released to the atmosphere. Several technologies have been developed for removing CO_2 from gas mixtures among them membrane separation, cryogenic fractionation, adsorption using molecular sieves, and chemical absorption. Chemical absorption is the most energy efficient of these separation techniques and is also the least expensive. As a result, most commercial CO_2-removal facilities use chemical absorption processes.

If nitrogen were not in the combustion products of coal-fired power plants, CO_2 capture would be greatly simplified and considerable less costly. Consequently, combustion schemes are

being developed that employ oxygen as the oxidizer instead of air. In such schemes, the exhaust streams will consist primarily of CO_2 and H_2O; a CO_2-rich stream that is ready for sequestration can be readily produced upon condensation of the water. Since combustion with oxygen (oxyfuel combustion) yields temperatures that are too high, flue gas recirculation can be used to moderate combustion temperatures.

Separating oxygen from air using an air-separation unit (ASU) is an energy intensive process. Techniques that enable combustion with oxygen without employing an ASU are therefore being developed. Chemical looping combustion is such a technology.

Chemical looping combustion (CLC) differs from conventional combustion processes in that air and fuel are never in direct contact. Instead, an oxygen carrier, typically a metal oxide such as Fe_2O_3 or CuO, is circulated between a fuel reactor and an air reactor to transfer the oxygen necessary for combustion of the fuel. In the fuel reactor, the fuel is oxidized to carbon dioxide and water and the metal oxide is reduced to the pure metal (or to a lower oxidation state). In the air reactor, the metal (or the lower oxidation state metal oxide) is oxidized back to its fully oxidized state. The following global reactions reflect the overall course of reaction:

$$\text{Fuel Reactor:} \quad M_xO_y + C_aH_b \rightarrow \tfrac{x}{x'} M_{x'}O_{y'} + \tfrac{b}{2} \cdot H_2O + a \cdot CO_2 \tag{1}$$

$$\text{Air Reactor:} \quad \tfrac{x}{x'} M_{x'}O_{y'} + \tfrac{n}{2} \cdot (O_2 + 3.76 \cdot N_2) \rightarrow M_xO_y + 1.88n \cdot N_2 \tag{2}$$

where M_xO_y is the metal oxide, C_aH_b is the hydrocarbon fuel, $n = b/2 + 2a$, and $y' = \frac{x'}{x}(y - n)$. Reaction (1) is often endothermic (depending on the metal oxide used), while reaction (2) is exothermic. The net heat release is the same as that with the conventional combustion of the fuel in air. Work is extracted from the hot, nitrogen-rich stream that exits the air reactor. Work can also be extracted from the hot products stream that exits the fuel reactor when a metal oxide is selected for which reaction (1) is exothermic.

The advantage of CLC is that the exhaust gas from the fuel reactor consists primarily of CO_2 and H_2O, essentially free of nitrogen-containing species. With little additional energy requirements, a pure stream of CO_2 can be readily produced [1]. Other technologies for CO_2 separation typically consume energy so that the overall thermal efficiency is generally lowered by 12-19% [2]. In contrast, theoretical models of CLC with Fe_2O_3 and natural gas have demonstrated thermal efficiencies that are commensurate with other advanced fossil fuel power cycles [3].

In our investigation of CLC, we have selected CuO as the oxygen carrier. Based on literature surveys and our own systems thermodynamic analyses, in comparison to several other potential oxygen carriers (Fe_2O_3, NiO, BaO_2, Mn_2O_3, and SrO_2), CuO exhibits advantages with respect to the fuel-to-metal oxide mass ratio required for complete combustion, bed operating temperatures and pressures, toxicity, availability, handling, and cost [4]. The only potential undesirable product formed is Cu_2S, however it is not yet known if its formation rate is high enough at the conditions in the fuel reactor to be problematic. Also, the metal oxide can be regenerated at modest temperatures and pressures. In addition, CuO can be reduced and regenerated multiple times without adverse effects on its reactivity.

Our overall efforts are directed at applying CLC technology to coal-fired and biomass-fired electric power plants, consequently we are concerned with the rates of oxidation of these solid fuels with CuO. However, before the oxidation rates can be characterized with respect to

temperature, pressure and reactive gas concentration, the rates of oxidation of CO, H_2 and CH_4 with CuO must be quantified. This is the objective of the work presented in this paper.

In the sections that follow, we present our experimental approach and show data obtained when CuO particles are exposed to CO, H_2 and CH_4. The reduced reaction mechanism developed for CuO/CO reacting systems is then introduced. We use the mechanism to examine some of the salient features of CO oxidation via CuO.

Experimental Approach

Flow reactor experiments

A batch-fed quartz reactor, illustrated in Fig. 1, was designed for the fuel oxidation experiments performed in this study. The reactor has a diameter of 1 inch and is 12 inches long. It contains a porous quartz plate located 3 inches from the reactor inlet to support the copper oxide bed. Gases enter the bottom of the reactor, percolate through the copper oxide bed and then exit through a port at the top of the reactor. The reactor was wrapped in insulation to minimize temperature gradients, which could induce thermal stresses and result in the reactor fracturing.

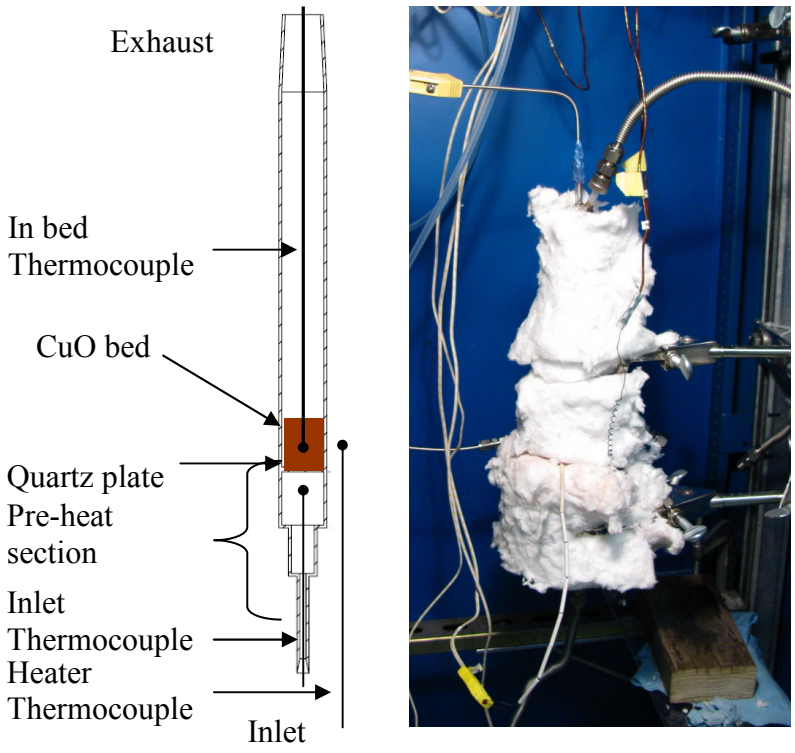

Figure 1. Bench Scale Flow Reactor

The reactor sits within a tubular heater capable of sustaining bed temperatures up to 1100 ˚C. Two inches of tubing upstream of the porous support plate as well as one inch of tubing after the metal oxide bed are located within the domain of the heater. The section of tubing prior to the quartz plate serves as a pre-heat section. The reactor has two ports at its outlet, one for the gases exiting the reactor and the other for insertion of a thermocouple that is used to measure the bed temperature.

Two additional thermocouples were used to measure temperatures during each experiment. The first thermocouple was located outside of the reactor and was used to control the heater temperature. The other thermocouple was located at the inlet to the reactor, just under the quartz plate and was used to measure the temperature of the gases entering the reactor. The location of the three thermocouples is illustrated in Fig. 1.

Rotometers were used to measure the flow rates of gases fed to the reactor. The rotometers was calibrated using a Varian digital flow meter.

In the flow reactor experiments, 5 to 10 grams of CuO were loaded into the quartz reactor and 150 to 300 milliliters per minute of the fuel (either CO, H_2 or CH_4) was flown into the reactor under a temperature ramp of 5 ˚C per minute up to 500 ˚C. The composition of the reactor exhaust gas was measured using a gas chromatograph (GC). The species monitored include CO, CO_2, H_2, CH_4, N_2, and O_2. For the experiments with hydrogen and methane, a cold trap was placed before the GC to prevent water from condensing in the tubing to the GC. For the flow reactor experiments, the overall rate of conversion of the CuO was determined from the flow rates of the gases fed to the reactor and the measured mole fractions of CO, CO_2, H_2 and CH_4 in the gases leaving, employing conservation relations.

Thermogravimetry experiments

Oxidation tests to determine the intrinsic chemical reactivity of the CuO to CO were performed in our pressurized thermogravimetric analyzer (TGA), an instrument that monitors the changes in the weight of a solid sample placed on its balance pan when the solid is exposed to specified conditions (temperature, pressure and reactive gas concentration) established in its reaction chamber. In our experimental procedure, about 30 mg of CuO (or Cu_2O) particles were placed in the TGA balance pan to minimize mass transfer effects. The particles were exposed to nitrogen at 298 K for 60 minutes before the temperature was increased to the specified reaction temperature. The particles experienced a dwell time of 60 minutes in nitrogen at the test temperature before the reactive gas was introduced into the reaction chamber. Weight change in the specified gaseous environment was monitored. The measured thermograms ($m(t)$ versus t data) were analyzed in order to determine the rates of the rate-limiting reactions that control the overall conversion rate of CuO to Cu during oxidation of the reactive gas.

Copper oxide particles

Copper II oxide (CuO) of 99.9% purity was purchased from Sigma Aldrich. Elemental copper (Cu) of 99.5% purity was also purchased for use in the copper oxidation (CuO regeneration) experiments. Prior to the experiments, the copper oxide particles were sieved to obtain particles in the 75 - 106 and 106 - 125 μm size ranges for testing. The size distributions for each size range were measured using a Coulter Multisizer, which counts the numbers of particles that are distributed into each of its 256 channels based on their size. All particles smaller than 10 microns were included in the 10-micron size channel. Results are shown in Fig. 2, where the measured number distributions were converted to fractional volume distributions. Since mass is proportional to the volume, these volume distributions emphasize the particle sizes containing most of the sample mass. Note that despite sieving, there are still a large number of particles having diameters less than 30 μm in each sample of particles.

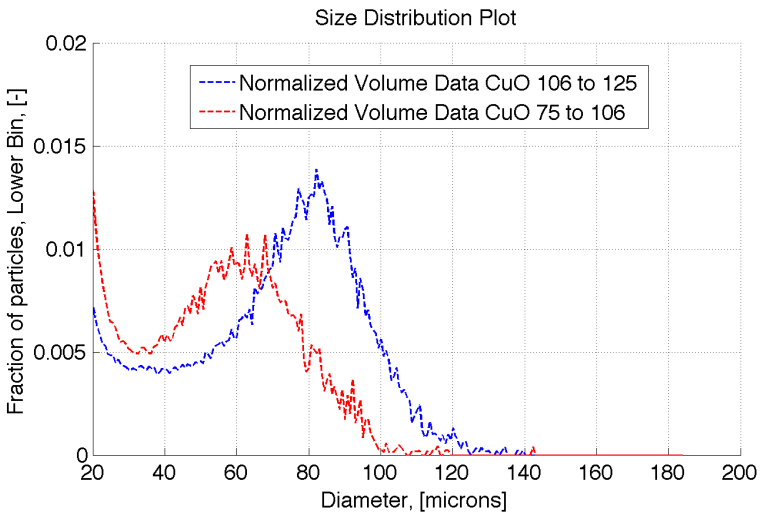

Figure 2. Size distributions of CuO particles

The unreacted and reacted CuO particles were also examined with a scanning electron microscope (SEM) and qualitatively analyzed via x-ray diffraction spectroscopy. Representative results are shown in the figures below. In the SEM images shown in Fig 3, the morphological change to the copper oxide particle as a result of a reduction cycle is evident. Despite the physical change of the surface as a result of CuO reduction, the specific surface area and size of each of the particles is about the same. Measurements of surface areas of the copper oxide and elemental copper particles were performed in our TGA, and both resulted in mass specific surface areas of about 1 m^2/gram. The Brunauer-Emmett-Teller (BET) [5] approach was used in the analysis of gas adsorption weight data to determine the surface areas. Carbon dioxide was used as the adsorption gas, and adsorption tests were performed at 296 K and 10 atm. A value of 22.2 $Å^2$ was used for the molecular cross section of CO_2 [6].

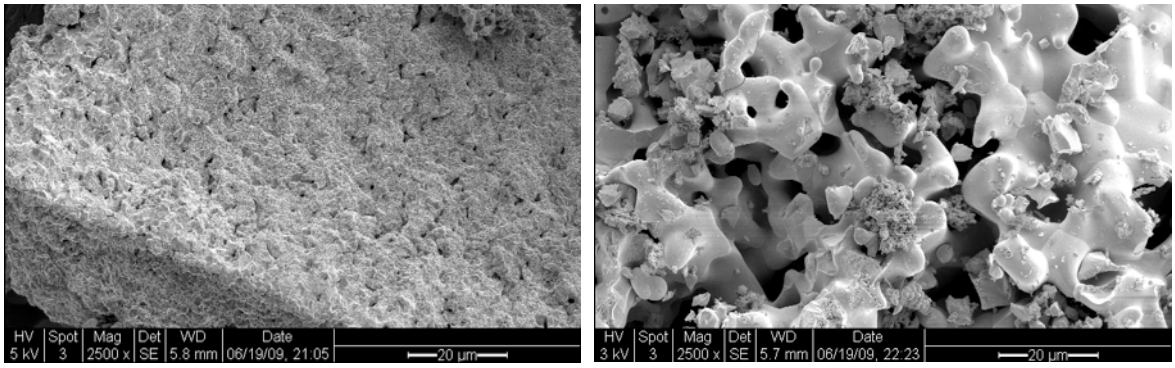

Figure 3. SEM images of the surfaces of unreacted (left) and reacted (right) CuO particles.

The X-ray diffraction tests were used to confirm the copper oxide species present in particles during an experiment. Shown in the left panel of Fig. 4 are data from the unreacted (raw) copper oxide sample used in the experiments along with reference X-ray diffraction data for CuO, and shown in the panel on the right are data from a partially reduced copper oxide sample along with reference X-ray diffraction data for Cu_2O. The partially reduced CuO sample was

actually obtained in some of our experiments with corn stover as the fuel. These data suggest a metal oxide reduction sequence of CuO to Cu_2O to Cu.

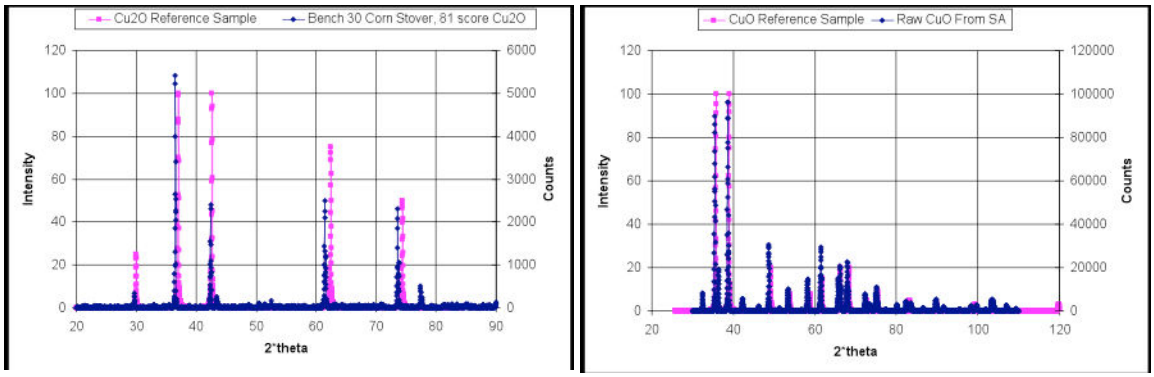

Figure 4: XRD spectra of unreacted (left) and partially reacted (right) CuO particles

Theoretical Approach

Copper Oxide Particle Conversion Model

Based on the volume-to-surface ratio, with an apparent density of 6.31 g/cm^3 and a specific surface area of about 1 m^2/g, the mean radius of pores inside a CuO particle is of the order 0.06 μm. Pores as large as 0.5 μm were noted in some of our SEM images. At diffusion-limited conversion rates for CuO particles exposed to 100% CO at temperatures less than 1000 ˚C, when account is made for both bulk and Knudsen diffusion inside pores of this size, the Thiele modulus is estimated to be less than 2 for particles less than 200 μm in diameter. For such values of the Thiele modulus, the effectiveness factor is greater than 0.8 for reaction orders near unity. Since CuO particles react at rates less than the diffusion-limited rates at temperatures less than 1000 ˚C, it can be assumed that the reactive gases essentially totally penetrate copper oxide particles having diameters less than 200 μm. There are insignificant mass transport effects limiting the CuO conversion rates; reaction takes place throughout the particle volumes. For example, the peak conversion rate observed in a test in our TGA when pulverized CuO particles were exposed to 100% CO at 400˚C was about four times less than the diffusion-limited rate. The Thiele modulus calculated using the measured rate was 0.87, which yields an effectiveness factor of 0.95 assuming first order reaction. Our model is developed for such cases, *i.e.,* for CuO particles less than 200 μm in size exposed to reactive gas environments at temperatures less than 1000 ˚C.

As the copper oxide particle reacts with the reactive gas, CuO is reduced to Cu_2O, which is reduced to Cu. During the course of reaction, the density of the solid particle varies from 6.31 g/cm^3 for CuO, to 6.0 g/cm^3 as Cu_2O is formed, to 8.94 g/cm^3 as Cu is formed. As oxygen atoms are removed from the copper oxide matrix, there are lattice rearrangements that result in overall particle apparent density and size changes. To account for these changes during reaction, power-law relations between mass density and diameter are used. During the transition from CuO to Cu_2O

$$\left(\frac{m}{m_0}\right)^{\alpha} = \frac{D}{D_0} \quad and \quad \left(\frac{m}{m_0}\right)^{\beta} = \frac{\rho}{\rho_0} \tag{1a}$$

where D_0 and ρ_0 are the initial diameter and density, respectively, of the CuO particle. For the transition from Cu_2O to Cu

$$\left(\frac{m}{m_{Cu_2O}}\right)^{\alpha'} = \frac{D}{D_{Cu_2O}} \quad and \quad \left(\frac{m}{m_{Cu_2O}}\right)^{\beta'} = \frac{\rho}{\rho_{Cu_2O}} \tag{1b}$$

where D_{Cu_2O} and ρ_{Cu_2O} are the diameter and density, respectivey, of the particle at 50% conversion, when the CuO particle has been reduced to a Cu_2O particle. The parameters α and β are conversion mode parameters for the CuO to Cu_2O transition and α' and β' are conversion mode parameters for the Cu_2O to Cu transition. Since particles are assumed to be spherical, $3\alpha + \beta = 1$ and $3\alpha' + \beta' = 1$. With these relations and the known density ratios for Cu_2O and CuO particles and for Cu_2O and Cu particles, the conversion mode parameters were determined: $\alpha = 0.175$, $\beta = 0.475$, $\alpha' = 1.454$, and $\beta' = -3.363$. Shown in Fig. 5 are the calculated variations in size and density employing these conversion mode parameters. The plots indicate that a 100-micron diameter CuO particle (with density 6.31 g/cm^3) would be reduced to about 98 μm at 50% conversion (with density 6.0 g/cm^3) and to about 83 μm at 100% conversion (with density 8.94 g/cm^3).

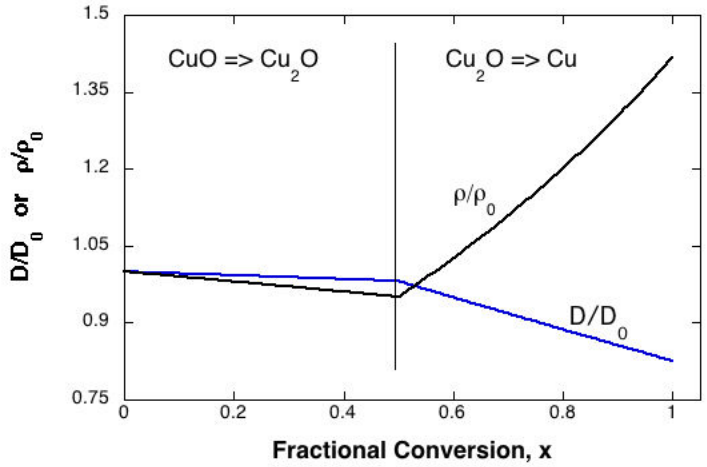

Figure 5: Variations in copper oxide particle size and density during reaction

Overall mass conversion rate per unit external surface area

During the reduction of CuO to Cu_2O, the rate of change in the mass of the copper oxide particle due to chemical reaction is found by differentiating the equations presented in Eqs. (1a):

$$\frac{dm}{dt} = \left[\frac{\pi\rho_0 D_0^3}{6(\alpha+\beta)}\left(\frac{D}{D_0}\right)^{1/\alpha}\frac{1}{D}\frac{dD}{dt} + \frac{\pi\rho_0 D_0^3}{6(\alpha+\beta)}\left(\frac{\rho}{\rho_0}\right)^{1/\beta}\frac{1}{\rho}\frac{d\rho}{dt}\right] \tag{2a}$$

The first term on the right-hand-side accounts for oxygen release and lattice rearrangements that result in diameter change and the second term accounts for oxygen release and the associated lattice rearrangements that result in density change. During the reduction of Cu_2O to CuO, the rate of change is given by

$$\frac{dm}{dt}=\left[\frac{\pi\rho_{Cu_2O}D_{Cu_2O}^3}{6(\alpha'+\beta')}\left(\frac{D}{D_{Cu_2O}}\right)^{1/\alpha'}\frac{1}{D}\frac{dD}{dt}+\frac{\pi\rho_{Cu_2O}D_{Cu_2O}^3}{6(\alpha'+\beta')}\left(\frac{\rho}{\rho_{Cu_2O}}\right)^{1/\beta'}\frac{1}{\rho}\frac{d\rho}{dt}\right] \tag{2b}$$

The overall mass conversion rate per unit external surface area (q_{ov}, in kg/m^2-s) is defined as follows:

$$q_{ov}\equiv-\frac{1}{\pi D^2}\frac{dm}{dt} \tag{3}$$

Combining Eqs. (2a) and (3) yields the following expression for the over mass conversion rate during the reduction of CuO to Cu_2O:

$$q_{ov}=-\left[\frac{\rho_0}{6(\alpha+\beta)}\left(\frac{D}{D_0}\right)^{(1/\alpha-3)}\frac{dD}{dt}+\frac{D_0^3}{6(\alpha+\beta)D^2}\left(\frac{\rho}{\rho_0}\right)^{(1/\beta-1)}\frac{d\rho}{dt}\right] \tag{4}$$

Defining the second term on the right-hand-side as R_{int}, the internal reaction rate per unit external surface area (in kg/m^2-s), q_{ov} can be rewritten as

$$q_{ov}=\left[\frac{\alpha}{\beta}+1\right]R_{\text{int}} \tag{5}$$

where

$$R_{\text{int}}=\frac{D_0^3}{6(\alpha+\beta)D^2}\left(\frac{\rho}{\rho_0}\right)^{(1/\beta-1)}\frac{d\rho}{dt} \tag{6}$$

The internal reaction rate is evaluated at the reactive gas partial pressure at the external surface of the particle, $P_{i,ex}$, which is assumed to be uniform throughout the particle. Expressions analogous to the relations given above apply during the reduction of Cu_2O to Cu.

The reactive gas must diffuse to the outer surface of the copper oxide particle. Assuming that there is no reaction in the boundary layer surrounding the particle, the mass flux of the reactive gas (J_i, in kg/m^2-s) at the particle's outer surface can be expressed as

$$J_{i,ex}=\frac{2D_i\hat{M}_i}{\hat{R}TD}\left(P_{i,\infty}-P_{i,ex}\right) \tag{7}$$

where D_i and $\hat{M}_i$ are the bulk diffusion coefficient (in m^2/s) and molecular weight (in kg/kmol), respectively, of the reactive gas; T is the particle temperature (in K); and $P_{i,\infty}$ is the partial pressure (in kPa) of the reactive gas in the ambient.

Now, for each mole of reactive gas that diffuses to the particle, ν_i moles of CuO (or Cu_2O) are reduced. Thus,

$$q_{ov}=\nu_i J_{i,ex}/\hat{M}_i=\frac{2D_i\nu_i\hat{M}_{CuO}}{\hat{R}TD}\left(P_{i,\infty}-P_{i,ex}\right)\equiv k_{diff}\left(P_{i,\infty}-P_{i,ex}\right) \tag{8}$$

where k_{diff} is the diffusional reaction rate coefficient. Combining Eqs. (5) and (8) yields the following expression, which applies as CuO is reduced to Cu_2O:

$$\left[\frac{\alpha}{\beta}+1\right]R_{\text{int}}=k_{diff}\left(P_{i,\infty}-P_{i,ex}\right) \tag{9a}$$

Since R_{int} is evaluated at $P_{\text{i,ex}}$, the only unknown in this equation is $P_{\text{i,ex}}$. The value so determined can be used in either Eq. (5) or (8) to evaluate q_{ov}. As Cu_2O is reduced to Cu, the following relation applies

$$\left[\frac{\alpha'}{\beta'}+1\right]R_{\text{int}} = k_{diff}\left(P_{i,\infty} - P_{i,ex}\right) \tag{9b}$$

CuO conversion times under kinetically limited reaction rates

At sufficiently low temperatures, the overall particle conversion rate is limited solely by the effects of chemical reaction, and the partial pressure of the reactive gas at the particle's outer surface is essentially the same as that in the ambient. In such cases, during conversion from CuO to Cu_2O, the overall mass conversion rate per unit external surface area is approximately given by

$$q_{ov} = \left[\frac{\alpha}{\beta}+1\right]R_{\text{int}}(P_{i,\infty}) \tag{10a}$$

and during conversion from Cu_2O to Cu by

$$q_{ov} = \left[\frac{\alpha'}{\beta'}+1\right]R_{\text{int}}(P_{i,\infty}) \tag{10b}$$

Here, $R_{\text{int}}(P_{i,\infty})$ indicates that the reaction rate is to be evaluated at the partial pressure of the reactive gas in the ambient. These equations apply only under kinetically limited reaction rates, under conditions when there are no mass transport effects limiting the conversion rates. The experiments undertaken in this study to determine kinetic parameters were made under such conditions.

The following equation applies during the reduction of CuO to Cu_2O under kinetically controlled reaction rates:

$$\frac{dm}{dt} = \pi D^2 q_{ov} = \pi D^2\left[\frac{\alpha}{\beta}+1\right]R_{\text{int}}(P_{i,\infty}) = \pi D_0^2\left(\frac{m}{m_0}\right)^{2\alpha}\left[\frac{\alpha}{\beta}+1\right]R_{\text{int}}(P_{i,\infty}) \tag{11}$$

Separating variables and integrating yields the following expression for the relationship between time and m/m_0:

$$t = \frac{\rho_0 D_0}{6(-2\alpha+1)(\alpha/\beta+1)R_{\text{int}}(P_{i,\infty})}\left[1-\left(m/m_0\right)^{(-2\alpha+1)}\right] \tag{12}$$

In terms of conversion, $x = (m_0 - m)/(m_0 - m_{\text{final}}) = (1 - m/m_0)/(1 - m_{\text{final}}/m_0)$, where $m_{final}/m_0 = \hat{M}_{Cu}/\hat{M}_{CuO}$, the above expression can be rewritten as

$$t = \frac{\rho_0 D_0}{6(-2\alpha+1)(\alpha/\beta+1)R_{\text{int}}(P_{i,\infty})}\left[1-\left(1-x(1-\hat{M}_{Cu}/\hat{M}_{CuO})\right)^{(-2\alpha+1)}\right] \tag{13}$$

This equation applies only up to 50% conversion, during the reduction of CuO to Cu_2O. For extents of conversion greater than 50%, during the reduction of Cu_2O to Cu,

$$t = t_{50\%} + \frac{\rho_{Cu_2O} D_0\left(\hat{M}_{Cu_2O}/2\hat{M}_{CuO}\right)}{6(-2\alpha'+1)(\alpha'/\beta'+1)R_{\text{int}}(P_{i,\infty})}\left[1-\left(\frac{m/m_0}{\left(\hat{M}_{Cu_2O}/2\hat{M}_{CuO}\right)}\right)^{(-2\alpha'+1)}\right] \tag{14}$$

where the time for 50% conversion, $t_{50\%}$, is given by

$$t_{50\%} = \frac{\rho_0 D_0}{6(-2\alpha+1)(\alpha/\beta+1)R_{\text{int}}(P_{i,\infty})}\left[1-\left(\hat{M}_{Cu_2O}/2\hat{M}_{CuO}\right)^{(-2\alpha+1)}\right] \tag{15}$$

In terms of conversion,

$$t = t_{50\%} + \frac{\rho_{Cu_2O} D_0\left(\hat{M}_{Cu_2O}/2\hat{M}_{CuO}\right)}{6(-2\alpha'+1)(\alpha'/\beta'+1)R_{\text{int}}(P_{i,\infty})}\left[1-\left(\frac{1-x\left(1-\hat{M}_{Cu}/\hat{M}_{CuO}\right)}{\left(\hat{M}_{Cu_2O}/2\hat{M}_{CuO}\right)}\right)^{(-2\alpha'+1)}\right] \tag{16}$$

Equations (13) and (16) give the time required to reach a specified extent of conversion under imposed conditions of temperature, pressure and reactive gas partial pressure. Note that the conversion time increases with the size of the CuO particle.

CO-CuO reaction mechanism

An equilibrium analysis was performed in order to determine the temperature at which CuO starts to dissociate. This is relevant in determining the initiation chemical reaction pathways for copper oxide conversion. The results from the analysis, illustrated in Fig. 6, imply that CuO dissociation does not begin until about 600 ˚C. The calculations also indicate little Cu formation at temperatures less than 1000 ˚C; the CuO is thermally reduced primarily to Cu_2O at these relative low temperatures. The data in the figure are measurements of the total mass on the balance pan of our TGA when CuO particles were heated in argon under a temperature ramp of 5˚C per minute. The agreement depicted confirms our analytical approach.

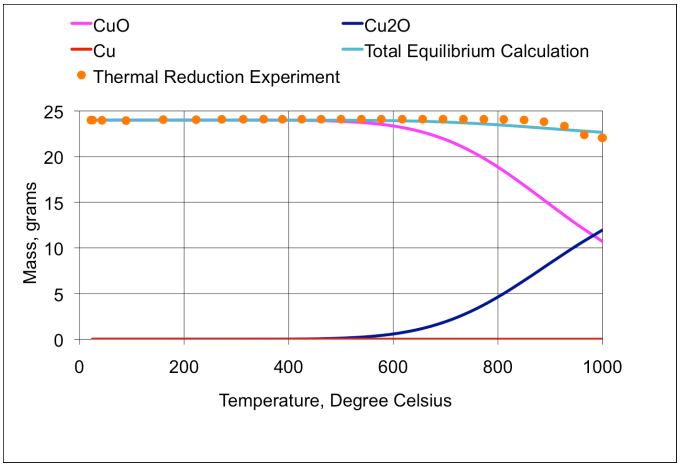

Figure 6. Equilibrium analysis of the thermal dissociation of CuO

Since reactions between CuO and CO were found to commence at temperatures below the dissociation temperature of CuO, it was assumed that the reacting system was initiated by CO adsorption at copper sites within the solid CuO matrix. It was also assumed that CO adsorption occurred at Cu_2O and Cu sites. In light of these assumptions, the following chemical reaction mechanism was developed to describe the reacting system:

$$CuO + CO \Leftrightarrow CuO(CO) \tag{R.1}$$

$$CuO(CO) \rightarrow Cu + CO_2 \tag{R.2}$$

$$CuO + CuO(CO) \rightarrow Cu_2O + CO_2 \tag{R.3}$$

$$Cu_2O + CO \Leftrightarrow Cu_2O(CO) \tag{R.4}$$

$$Cu_2O(CO) \rightarrow 2Cu + CO_2 \tag{R.5}$$

$$Cu_2O \Leftrightarrow Cu + CuO \tag{R.6}$$

$$Cu + CO \Leftrightarrow Cu(CO) \tag{R.7}$$

The species CuO(CO), $Cu_2O(CO)$, and Cu(CO) are adsorbed surface species, copper sites having adsorbed CO. Only those reactions that remove an oxygen atom from the bulk copper matrix are considered to be irreversible. These are the reactions that form CO_2 and hence are the reactions that govern the copper conversion rate. On a molar basis, the intrinsic chemical reactivity of CuO to CO (the rate of oxidation of CO by CuO) is given by

$$\hat{R}_{CuO/CO} = \hat{R}_2 + \hat{R}_3 + \hat{R}_5 = k_2\left[CuO(CO)\right] + k_3\left[CuO(CO)\right]\left[CuO\right] + k_5\left[Cu_2O(CO)\right] \tag{17}$$

where $\hat{R}_j$ is the rate of reaction j, (in mol/m^2-s), k_j is the reaction rate coefficients for reaction j, and the bracketed terms denote the concentrations of the species indicated.

Based on the mechanism, the adsorbed species concentrations are governed by the following differential equations:

$$\frac{d\left[CuO(CO)\right]}{dt} = \hat{R}_1 - \hat{R}_2 - \hat{R}_3 = k_{1f}\left[CuO\right]\left[CO\right] - k_{1r}\left[CuO(CO)\right] - k_2\left[CuO(CO)\right] - k_3\left[CuO(CO)\right]\left[CuO\right] \tag{18}$$

$$\frac{d\left[Cu_2O(CO)\right]}{dt} = \hat{R}_4 - \hat{R}_5 = k_{4f}\left[Cu_2O\right]\left[CO\right] - k_{4r}\left[Cu_2O(CO)\right] - k_5\left[Cu_2O(CO)\right] \tag{19}$$

and

$$\frac{d\left[Cu(CO)\right]}{dt} = \hat{R}_7 = k_{7f}\left[Cu\right]\left[CO\right] - k_{7r}\left[Cu(CO)\right] \tag{20}$$

The concentrations of CuO, Cu_2O and Cu are governed by the following differential equations:

$$\frac{d\left[CuO\right]}{dt} = -\hat{R}_1 - \hat{R}_3 + \hat{R}_6 = -k_{1f}\left[CuO\right]\left[CO\right] + k_{1r}\left[CuO(CO)\right] - k_3\left[CuO(CO)\right]\left[CuO\right] + k_{6f}\left[Cu_2O\right] - k_{6r}\left[Cu\right]\left[CuO\right] \tag{21}$$

$$\frac{d\left[Cu_2O\right]}{dt} = \hat{R}_3 - \hat{R}_4 - \hat{R}_6 = k_3\left[CuO(CO)\right]\left[CuO\right] - k_{4f}\left[Cu_2O\right]\left[CO\right] + k_{4r}\left[Cu_2O(CO)\right] - k_{6f}\left[Cu_2O\right] + k_{6r}\left[Cu\right]\left[CuO\right] \tag{22}$$

and

$$\frac{d\left[Cu(CO)\right]}{dt} = \hat{R}_7 = k_{7f}\left[Cu\right]\left[CO\right] - k_{7r}\left[Cu(CO)\right] \tag{23}$$

In the above expressions, for a surface species, $[X_i]$ is in units of mol/m^2 of surface and for a gas-phase species, $[X_i]$ is in units of mol/m^3 of fluid.

In our approach, we solve for the surface species site fractions (θ_i) instead of the concentrations of the surface species, where the site fractions are defined as

$$\theta_i = [X_i]\lambda_i / (S/N_{av}) \tag{24}$$

Here, λ_i is the number of sites that species *i* occupies, *S* is the total site density (the number of copper sites per m^2 surface), and N_{av} is Avogadro's number. Since the site fractions sum to unity, we determine θ_{CuO} by difference ($\theta_{CuO} = 1 - \theta_{Cu2O} - \theta_{Cu} - \theta_{CuO(CO)} - \theta_{Cu2O(CO)} - \theta_{Cu(CO)}$) instead of integrating Eq. (21) (when written in terms of the site fractions).

In terms of the site fractions, the mass reactivity of CuO to CO is given by

$$R_{CuO/CO} = \hat{M}_{CuO}\hat{R}_{CuO/CO} = \hat{M}_{CuO}\left(\frac{S}{N_{av}}\right)\left\{k_2\theta_{CuO(CO)} + k_3\left(\frac{S}{N_{av}}\right)\theta_{CuO(CO)}\theta_{CuO} + \frac{1}{2}k_5\theta_{Cu_2O(CO)}\right\} \tag{25}$$

The above expression, when evaluated at the conditions existing at the outer surface of the CuO particle, yields R_{int}, which is used in several of the equations presented above, in particular in Eqs. (9) – (16).

Discussion of Results

Flow reactor tests

Shown in Figs. 7 – 9 are results of experiments performed in the flow reactor when 5 to 10 grams of CuO particles having diameters less than 125 μm were loaded into the quartz reactor and either 100% CO, a 20%/80% mixture of H_2 and Ar, or 99% CH_4 (balance N_2) was introduced at a flow rate of 150 to 310 milliliters per minute under a temperature ramp of 5˚C per minute up to 500˚C. It is noted that with each of the gaseous fuels, the chemical reactions are initiated well below 600˚C. Evidence of exothermic chemical reactions can be noted by the deviation in the temperature profile from linearity. When exposed to 100% CO (Fig. 7), there is a large deviation in the temperature profile that begins at a temperature below 100 ˚C. The CO was admitted into the flow reactor at a rate of 301 mL/min. The 27.45 g of copper oxide that was placed in the reactor was completely reduced to Cu by the time the temperature has increased to about 250˚C.

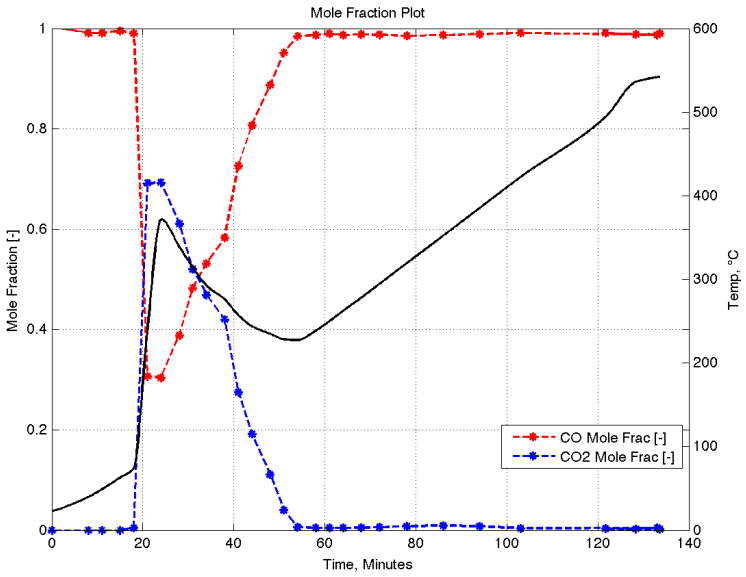

Figure 7. Carbon monoxide oxidation via CuO

When exposed to 20% H_2 in argon (Fig. 8), reaction is initiated at a temperature of about 125˚C. In this test, the gases entered the reactor at a rate of 271 mL/min, and 13.1 g of CuO was loaded into the reactor. The deviation in the temperature profile is not as distinct as it was in 100% CO due to the effects of dilution. Note that there was sufficient CuO loaded into the reactor to completely consume the hydrogen supplied. The H_2 mole fraction was reduced to near zero levels by the time the temperature was increased to about 325˚C.

When exposed to 99% CH_4 in N_2 (Fig. 9), reaction is initiated at a temperature of about 375˚C, a higher initiation temperature than observed with either CO or H_2 but still less than the temperature at which CuO thermally decomposes. Only 6.67 g of CuO were loaded into the reactor for this test; the gas was admitted at a rate of 296 mL/min. The temperature ramp rate was 5˚C per minute. The CH_4 oxidation process seems to be more complex than either CO or H_2 oxidation. At the time of the initial drop in the methane mole fraction, there is CO_2 formation. The decrease in the CH_4 mole fraction is essentially tracked by an increase in the CO_2 mole fraction up to the time the temperature reaches about 400˚C, suggesting complete methane oxidation. As temperature is increased above 400˚C, H_2 and modest amounts of CO are observed. The CO and CO_2 mole fractions do not account for the decrease in the methane mole fraction, suggesting carbon formation. The H_2 mole fraction initially increases but peaks at about 600 ˚C, when oxygen atoms released from the copper oxide particle begins and gas-phase H_2 oxidation occurs. Once all the oxygen atoms have been released, the H_2 mole fraction starts to increase as the methane thermally decomposes at temperatures above 800˚C. The heaters were turned off at the time the temperature starts to drop just before 240 minutes into the test.

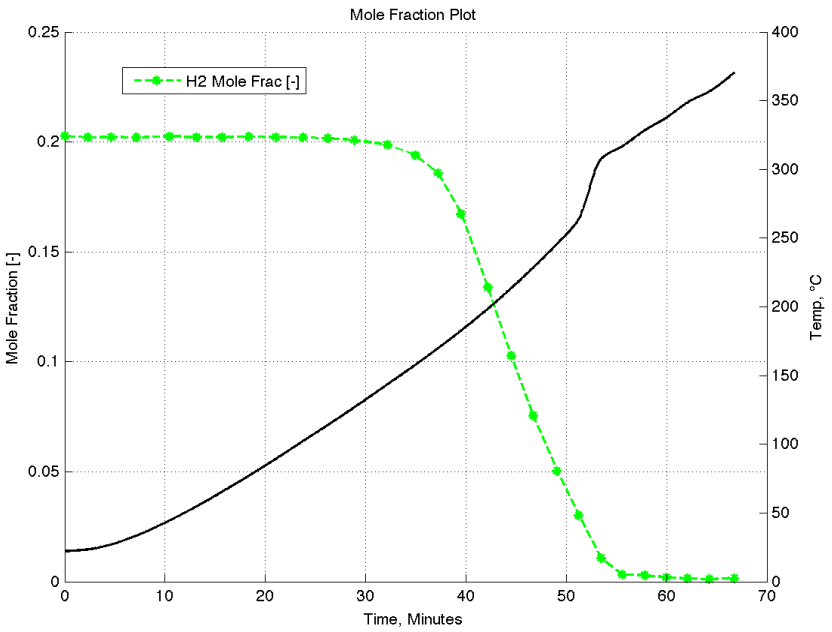

Figure 8. Hydrogen oxidation via CuO

The flow reactor tests demonstrate that the oxidation process begins with the reactive gas contacting the CuO surface. Oxygen primarily leaves the particles bond in CO_2 and H_2O. The test with methane indicates a potential concern, cracking of the CH_4. Above stoichiometric quantities of CuO are required to circumvent carbon formation during CLC applications.

Copper oxide regeneration

Shown in Fig. 10 are results obtained in a test to examine Cu oxidation in air. In this test, 27.45 g of Cu was loaded into the reactor and air was admitted at a rate of 307 mL/min, heated at a rate of 5˚C to 500˚C. The reaction began at a temperature of about 125˚C. By the time the temperature reached 475˚C, the oxygen was essentially completely consumed by the copper. Once the Cu was completely oxidized, the O_2 mole fraction increased back to its value in air, 0.21. This test was conducted under the same conditions as the CO oxidation test with CuO. The same amount of solid was loaded into the reactor and the same gas flow rate and heating rate were used. As noted, there is no mismatch in the characteristic times for CuO oxidation and CuO regeneration.

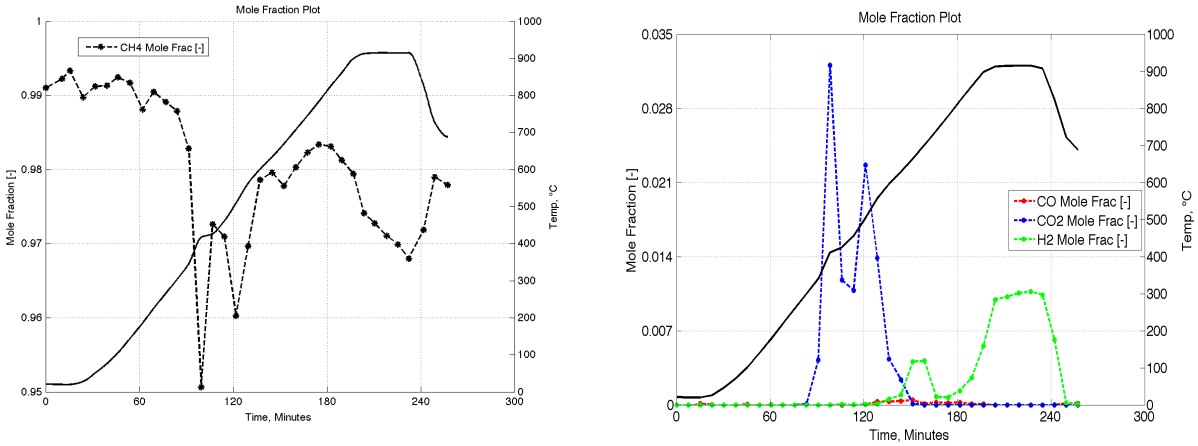

Figure 9. Methane oxidation via CuO

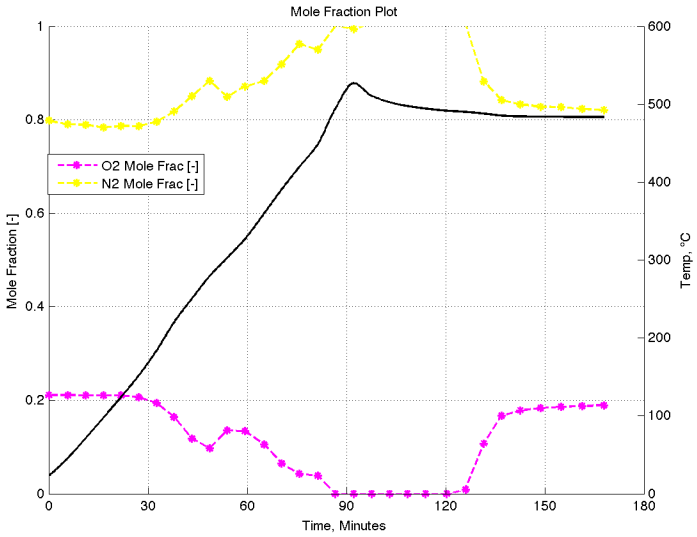

Figure 10. Copper Oxidation

Thermogravimetric tests

Thermogravimetric tests were undertaken to obtain data needed to determine the kinetic parameters that describe the reduction rates of CuO when exposed to CO. Twenty to thirty

milligrams of CuO or Cu_2O particles were placed in the TGA balance pan and weight was monitored for up to 600 min (in some cases) in the conditions established in the TGA reaction chamber. After drag and buoyancy corrections, the weight-versus-time data were analyzed to determine the extent of conversion and as a function of conversion, the quantity 1/m dm/dt, a quantity that is proportional to the reaction rate. Shown in Figs. 11 and 12 are results obtained when CuO particles were placed on the balance pan and the reactive gas consisted of 1.6% CO in nitrogen and 100% CO at 400˚C. As noted in Fig. 11, the extent of reaction does not reach 100%, the mass on the balance pan was never reduced to the level indicating all Cu. This is due to adsorbed CO on Cu. Also note that a quasi steady-state is reached in 100% CO in a relatively short time compared to the time it takes the reacting system to reach a steady state when there is only 1.6% CO. The quantity 1/m dm/dt is shown in Fig. 12. The rate is observed to vary with conversion and to increase with temperature.

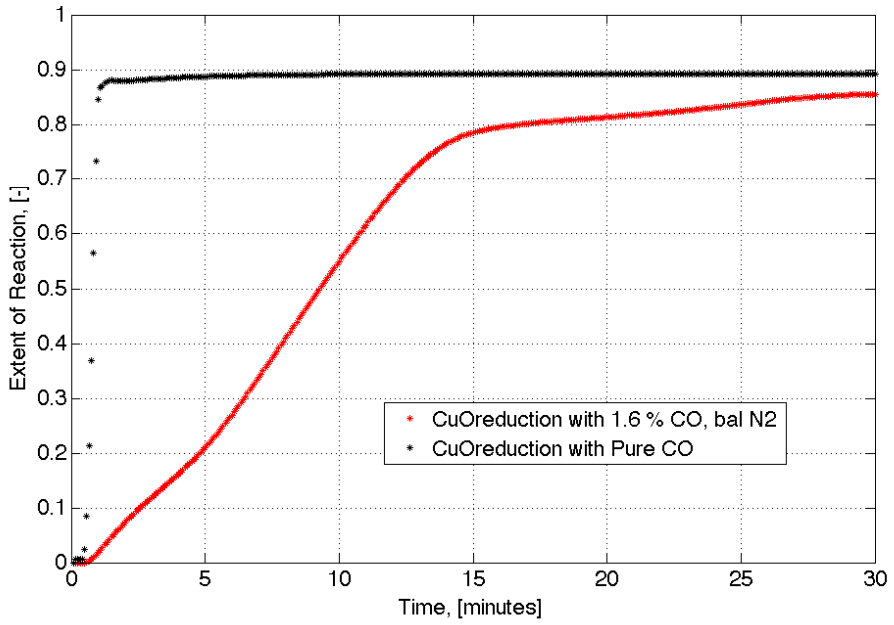

Figure 11. Extent of conversion as a function of time for CuO particles exposed to 1.6% and 100% CO at 400˚C at 1 atm

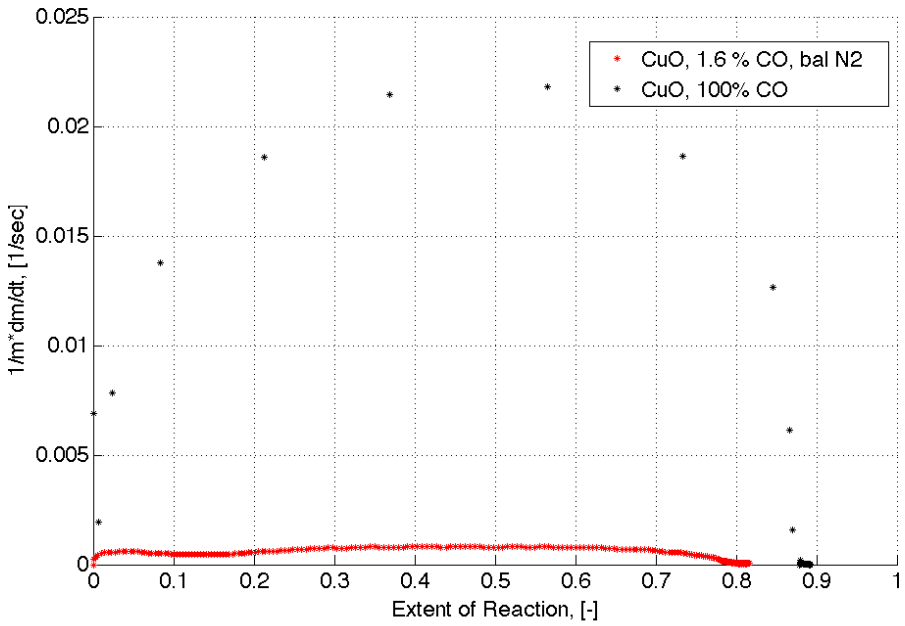

Figure 12. Conversion rate as a function of extent of conversion for CuO particles exposed to 1.6% and 100% CO at 400 ˚C and 1 atm

Rate coefficients for the reactions in the reaction mechanism being developed are determined from the type data presented in Fig. 12. Based on the mechanism,

$$\frac{1}{m}\frac{dm}{dt} = -\hat{M}_{CO}\hat{R}_1 + \hat{M}_{CO_2}\hat{R}_2 + \hat{M}_{CO_2}\hat{R}_3 - \hat{M}_{CO}\hat{R}_4 + \hat{M}_{CO_2}\hat{R}_5 - \hat{M}_{CO}\hat{R}_7 \qquad (26)$$

where $\hat{R}_i$ is the molar rate of Reaction *i,* which is written in terms of rate coefficients k_i and the concentrations of the species involved in the reaction, as described above when discussing the reaction mechanism. Using a least squares procedure, k_i for each reaction is determined that minimizes the sum of the differences in the measured and calculated values of 1/m dm/dt at each extent of reaction. We have not yet been able to determine a set of kinetic parameters that describe all data sets. Activities are currently underway to determine Arrhenius parameters for the rate coefficients that describe all the experimental observations.

Conclusions

Experiments in a flow reactor and a TGA indicate that CuO is an effective oxygen carrier for the oxidation of CO, H_2 and CH_4. The experiments support the thermochemical equilibrium calculations that indicate that the CuO is relatively stable at temperatures below 600 ˚C, higher temperature being required for release of oxygen. With gaseous fuels such as H_2, CO and CH_4, carbon dioxide (CO_2) is observed at temperatures as low as 300 ˚C, indicating that the reactive gas initiates copper oxide decomposition.

A model for a CuO particle undergoing chemical reaction when exposed to a reactive gas environment has been developed that accounts for the changes in diameter and density that particles undergo as oxygen is released from the solid matrix. Thiele modulus calculations suggest that particles are nearly totally penetrated by the reactive gas, consequently, the model

assumes that the reactive gas concentration inside the particle is uniform. Reaction is initiated by the adsorption of CO at copper sites within the solid. A reduced heterogeneous reaction mechanism was developed to account for the observed conversion rates. Kinetic parameters that describe the rates of the reactions are being determined.

Acknowledgements

The authors would like to acknowledge the support from the California Energy Commission Grant 07-01-37 and Clean EnGen L.L.C.

References

1. Henrik, L.; M. Tobias; L. Anders. *Proceedings of the 33rd International Technical Conference on Coal Utilization & Fuel Systems* (2008).
2. Linssen, J.; P. Markewitz; D. Martinsen; M. Walbeck. *Bwk* 58 (7-8), 59-62 (2006).
3. Naqvi, R.; O. Bolland. *International Journal of Greenhouse Gas Control* 1(1), 19-30 (2007).
4. Touchton, G.; M. Zuzga. "Air Independent Internal Oxidation Steam Generator," Final Report, Energy Innovations Small Grant Program, Grant #07-05. Submitted for review, September 2009.
5. Brunauer, S.; Emmett, P. H.; Teller, E. *J., Am. Chem. Soc.* 60, 309-319 (1938).
6. Gregg, S. J.; Sing, K. S. W. *Adsorption, Surface Area and Porosity*, 2nd Ed. New York, Academic Press (1982).